High-Performance MC-CDMA Via Carrier Interferometry Codes

Balasubramaniam Natarajan, Carl R. Nassar, Steve Shattil, Marco Michelini, and Zhiqiang Wu

***Abstract*—This paper introduces the principles of interferometry to multicarrier code division multiple access (MC-CDMA). Specifically, we propose the use of MC-CDMA with novel carrier interferometry (CI) complex spreading codes. The CI/MC-CDMA method, applied to mobile wireless communication systems, offers enhanced performance and flexibility relative to MC-CDMA with conventional spreading codes. Specifically, assuming a frequency selective Rayleigh-fading channel, CI/MC-CDMAs performance matches that of orthogonal MC-CDMA using Hadamard–Walsh codes up to the MC-CDMA N user limit; and, CI/MC-CDMA provides the added flexibility of going beyond N users, adding up to $N-1$ additional users with pseudo orthogonal positioning. When compared to MC-CDMA schemes capable of supporting greater than N users, CI/MC-CDMAs performance exceeds that of MC-CDMA. Additionally, this new system is analyzed in the presence of phase jitters and frequency offsets and is shown to be robust to both cases.**

***Index Terms*—Carrier interferometry, complex sequences, frequency diversity, multicarrier code division multiple access (MC-CDMA).**

I. Introduction

MULTICARRIER code division multiple access (MC-CDMA) [1] has emerged as a powerful alternative to conventional direct sequence CDMA (DS-CDMA) [2] in mobile wireless communications. In MC-CDMA, each user's data symbol is transmitted simultaneously over N narrow-band subcarriers, with each subcarrier encoded with a -1 or $+1$ (as determined by an assigned spreading code). Multiple users are assigned unique, orthogonal (or pseudo-orthogonal) codes. That is, while DS-CDMA spreads in the time domain, MC-CDMA applies the same spreading sequences in the frequency domain.

When perfectly orthogonal code sequences are transmitted over slow, flat fading channels with perfect synchronization, the performance of DS-CDMA and MC-CDMA is equivalent, as the orthogonal multi-user interference vanishes completely. However, in reality, wide-band CDMA signals sent over multipath channels experience more severe channel distortions and the resulting channel dispersion (i.e., frequency selectivity) erodes the orthogonality of CDMA signals. In such cases, it turns out to be far more beneficial to harness the signal energy in the frequency domain (as in MC-CDMA) than in the time domain (as in DS-CDMA) [2].

Specifically, MC-CDMA receivers exploit frequency diversity in the frequency selective channel by separating carriers and then carefully recombining them, while DS-CDMA RAKE receivers use correlators to resolve multiple paths and create path diversity. The reasons MC-CDMA receivers outperform their DS-CDMA counterparts include: 1) in RAKE receivers, large interference results due to the presence of other users' signals from other paths as well as one's own signal from other paths and 2) in RAKE receivers, optimal combining of resolvable (correlated) paths is not a trivial problem; as a result, the typical (suboptimal) simplification assumes that interference in resolvable paths is independent, explaining the widespread use of (the suboptimal) maximum ratio combining (MRC) in the RAKE receiver, e.g., [2]. On the other hand, in MC-CDMA, frequency selectivity results in a different attenuation on each subcarrier. Unlike DS-CDMA where paths are correlated, MC-CDMA subcarriers are orthogonal, enabling receivers to perfectly separate the subcarrier components by performing an FFT operation. Next, a recombining can be performed using weights corresponding to MRC [1] or the high-performance Weiner filtering [i.e., minimum mean square error combining (MMSEC)] (or some other optimal or suboptimal strategy). For these reasons, MC-CDMA demonstrates performance gains relative to DS-CDMA.

Interferometry [3], a classical method in experimental physics, refers to the study of interference patterns resulting from the superpositioning of waves. The presence of distinct peaks and nulls in the interference patterns has motivated the widespread use of interferometry. The ideas underlying interferometry lend themselves naturally to multiple access applications in telecommunications. For example, in antenna arrays supporting space division multiple access, electromagnetic (EM) waves are emitted simultaneously from multiple antenna elements and initial phases are chosen to ensure that interference patterns create a peak at the desired user location and nulls at the position of other users.

In this work, we apply the principles of interferometry to create a novel code set for MC-CDMA based on carrier interferometry. The idea here is that each user simultaneously transmits the N carriers of MC-CDMA, with carefully chosen phase offsets (spreading codes) that ensure a periodic mainlobe in the time domain (with sidelobe activity at intermediate times). When the superpositioning of one user's carriers creates a mainlobe in time, all other users are at the times of sidelobe activity (and, by careful positioning, can be made strictly orthogonal or pseudo-orthogonal to the user transmitting a mainlobe).

Manuscript received February 8, 2000; revised October 16, 2000.

B. Natarajan, C. R. Nassar, and Z. Wu are with the Department of Electrical and Computer Engineering, Colorado State University, Fort Collins, CO 80523-1373 USA (e-mail: nbalsu@engr.colostate.edu).

S. Shattil is with Idris Communication, Boulder, CO 80303 USA.

M. Michelini is with the Department of Electrical Engineering, Università di Firenze, Firenze 50139, Italy.

Publisher Item Identifier S 0018-9545(01)09173-3.

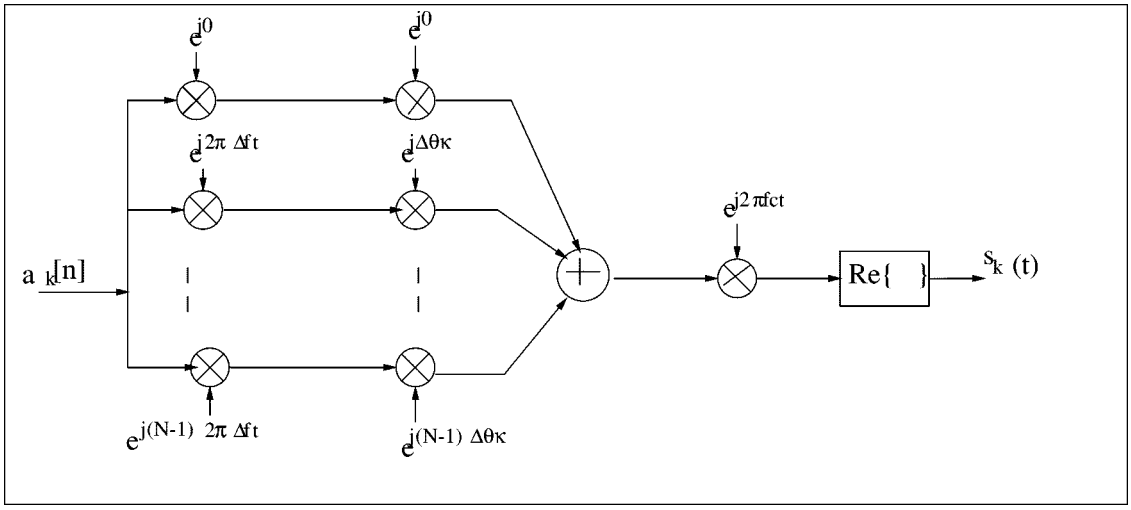

Fig. 1. CI/MC-CDMA transmitter for user k.

In this proposed innovation to MC-CDMA, we are replacing the use of spreading codes identical to those in DS-CDMA with spreading codes which create interferometry patterns among carriers. Hence, we call our proposed codes carrier interferometry codes (CI codes) and our proposed scheme carrier interferometry/MC-CDMA (CI/MC-CDMA). Already, there has been tremendous interest in the development of spreading codes (e.g., for DS-CDMA, see [4]–[7]; see [8] for an overview of MC-CDMA codes). In [4], a general set of complex valued spreading codes for DS-CDMA are proposed that provide a better compromise between auto and cross correlation properties relative to binary spreading codes. However, codes of length Nsupport a maximum of only $N-1$ users. In [5] and [6], a novel spread signature CDMA system is introduced where the length of the spreading code is far greater than the symbol duration. This technique is best suited to exploit temporal diversity in fast fading environments. Additionally, in [7], a multivalued set of orthogonal codes are constructed using wavelet and subband transform theories. In [8], a thorough analysis and comparison of existing MC-CDMA codes is presented; specifically, [8] examines the use of Hadamard Walsh, Gold, Orthogonal Gold, and Zadoff Chu sequences, in MC-CDMA systems. However, the DS-CDMA codes ([4]–[7]) and MC-CDMA codes [8] are designed to be either orthogonal, supporting N users (where N is the processing gain or code length), or pseudo-orthogonal, supporting greater than N users, at the cost of degraded performance. Furthermore, N, is limited to 2^n or $2^n \pm 1$ ($n \in I$). CI codes of length N introduced in this paper have a unique feature which allows the CI/MC-CDMA system to: 1) support N users orthogonally and 2) then, as system demand increases, codes can be selected to accommodate up to an additional $N-1$ users pseudo-orthogonally. Additionally, there is no restriction on the length N of the CI code (i.e., $N \in I$), making it more robust to the diverse requirements of wireless environments.

This work demonstrates the flexibility and the performance improvement achievable through CI/MC-CDMA. In frequency selective Rayleigh-fading channels, CI/MC-CDMAs performance matches that of orthogonal MC-CDMA using Hadamard–Walsh codes up to the MC-CDMA N user limit; and, CI/MC-CDMA provides the added flexibility of going beyond N users, adding up to $N-1$ additional users with pseudo orthogonal positioning. When compared to MC-CDMA schemes capable of supporting greater than N users, CI/MC-CDMAs performance exceeds that of MC-CDMA.

Section II discusses the CI/MC-CDMA codes and transmitter; Section III presents the channel and Section IV introduces the receiver structure. Section V provides performance results of the CI/MC-CDMA system with: a) perfect synchronization; b) phase jitters; and c) frequency offsets. A brief discussion of future work and conclusions follows in Section VI.

II. CI/MC-CDMA Signaling and Transmitter Model

The transmitter for the kth user in a CI/MC-CDMA system is shown in Fig. 1. Here, the kth user's spreading code corresponds to $(1, e^{j\Delta\theta_k}, e^{j2\Delta\theta_k}, \ldots, e^{j(N-1)\Delta\theta_k})$. The input data symbol is $a_k[n]$ where n denotes the nth bit interval and k denotes the kth user. It is assumed that $a_k[n]$ takes on values -1 and $+1$ with equal probability. The transmitted signal corresponding to the nth data bit of the kth user is

$$s_k(t) = \sum_{i=0}^{N-1} a_k[n] \cos(2\pi f_i t + i\Delta\theta_k) \cdot p(t - nT_b) \qquad (1)$$

where $f_i = f_c + i\Delta f$ and $p(t)$ is defined to be a Nyquist pulse for the bit in the interval 0 to T_b. As with traditional MC-CDMA, the Δfs are selected such that the carrier frequencies $\{f_i, i = 0, 1, \ldots, N-1\}$ are orthogonal to each other, typically $\Delta f = 1/T_b$, where T_b is the bit duration.

The transmitted signal can be expressed as

$$s_k(t) = [a_k[n] \cdot p(t - nT_b)] \cdot c_k(t) \qquad (2)$$

where $c_k(t)$ corresponds to the superpositioning of N equally spaced carriers, i.e.,

$$c_k(t) = \sum_{i=0}^{N-1} \cos(2\pi f_i t + i\Delta\theta_k). \qquad (3)$$

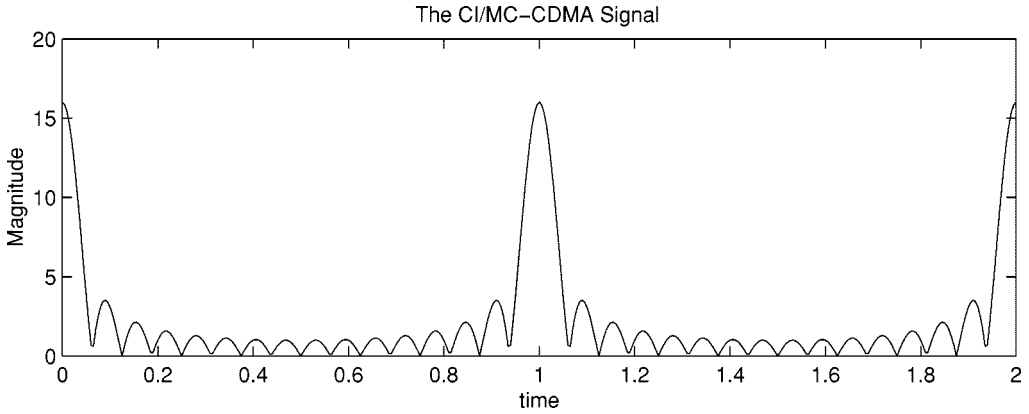

Fig. 2. Envelope of a CI/MC-CDMA signal.

This signal corresponds to a cosine waveform with frequency $f_c + ((N-1)/2)\Delta f$ and envelope

$$E_k(t) = \left| \frac{\sin\left(\frac{1}{2}N(2\pi\Delta f t + \Delta\theta_k)\right)}{\sin\left(\frac{1}{2}(2\pi\Delta f t + \Delta\theta_k)\right)} \right|. \tag{4}$$

Fig. 2 plots the envelope for $N = 16$ carriers, $T_b = 1$ s, and $\Delta\theta_k = 0$, demonstrating that the signal $c_k(t)$ is: 1) periodic with period $1/\Delta f = T_b$; 2) each period contains a mainlobe of duration $2/N\Delta f = 2T_b/N$ with the mainlobe positioned at time $nT_b + \Delta t_k = nT_b + \Delta\theta_k/2\pi\Delta f = nT_b + (\Delta\theta_k/2\pi)T_b$; 3) each period contains $N-1$ sidelobes of duration $1/N\Delta f = T_b/N$, where the lth sidelobe has maximum amplitude (normalized with respect to mainlobe amplitude) of $A(l) = 1/(N\sin(\pi/N)(l+(1/2))$.

The cross correlation (CC) between user k's signature waveform $c_k(t)$ [created using the spreading sequence $(1, e^{j\Delta\theta_k}, e^{j2\Delta\theta_k}, \ldots, e^{j(N-1)\Delta\theta_k})$] and user j's signature waveform $c_j(t)$ [created via the spreading sequence $(1, e^{j\Delta\theta_j}, e^{j2\Delta\theta_j}, \ldots, e^{j(N-1)\Delta\theta_j})$] can be shown to be

$$R_{k,j}(\tau) = \frac{1}{2\Delta f}\sum_{i=0}^{N-1}\cos(i(2\pi\Delta f\tau)) \tag{5}$$

$$R_{k,j}(\tau) = \frac{1}{2\Delta f}\cdot\frac{\sin\left(\frac{1}{2}N2\pi\Delta f\tau\right)}{\sin\left(\frac{1}{2}2\pi\Delta f\tau\right)} \cdot\cos\left(\frac{(N-1)}{2}2\pi\Delta f\tau\right) \tag{6}$$

where $\tau = \Delta t_k - \Delta t_j = (\Delta\theta_k - \Delta\theta_j)/2\pi\Delta f$. This CC term demonstrates $2(N-1)$ zeros:

- $N-1$ equally spaced zeros at $\{(k/N\Delta f), k = 1, 2, \ldots, N-1\}$ resulting from the $\sin(\cdot)/\sin(\cdot)$ term;
- $N-1$ equally spaced zeros at $\{((2k-1)/(2(N-1)\Delta f)), k = 1, 2, \ldots, N-1\}$ as a result of the $\cos(\cdot)$ term.

This indicates that for a given signature waveform $c_k(t)$ there exist $2(N-1)$ orthogonal signature waveforms $c_j(t)$. If N is even, $2(N-1)-1$ orthogonal signature waveforms exist because one of the zeros ($k = N/2$) is common to the two sets.

The existence of the first set of $N-1$ equally spaced zeros in $R_{k,j}(\tau)$ indicates that a CI/MC-CDMA system can simultaneously support N orthogonal signature waveforms (and, hence, N orthogonal users). The existence of a second set of zeros, equally spaced by time separation $(1/((N-1)\Delta f))$, indicates that we can place an additional $(N-1)$ signature waveforms at highly (but pseudo) orthogonal locations. [The first set of N orthogonal signature waveforms and the second set of $N-1$ signature waveforms are nearly orthogonal (pseudo-orthogonal)]. Hence, a CI/MC-CDMA system can support N orthogonal users and, additionally, if more users are to be accommodated, it can support these users pseudo-orthogonally by assigning up to $N-1$ pseudo-orthogonal signature waveforms. This flexibility is not found in the MC-CDMA codes available to date, where codes are chosen to support N orthogonal users *or* greater than N pseudo-orthogonal users.

It is important to note, as is evident from Fig. 2, that the peak to average power ratio (PAPR) and the dynamic range of the multicarrier waveform is high (as is typical of most multicarrier transmission schemes). An increased PAPR can result in reduced efficiency of the power amplifier, meaning that the average radiated power is reduced in order to avoid a nonlinear distortion in the transmitted signal. Also, an increased signal dynamic range implies the need for an increased range of linearity in the power amplifier. For these reasons, schemes to reduce PAPR/dynamic range have received a great deal of attention in MC-CDMA literature [9]–[12]. A short-term solution is found in the use of a predistortion filter that accounts for the nonlinearity of the power amplifier (e.g., [9], [10]). A long term solution is found in the use polyphase coded carriers where phase offset Θ_i, unique to the ith carrier but fixed for all users, is introduced to reduce PAPR and dynamic range (e.g., [11], [12]).

III. Channel Model

In this paper, we assume synchronicity between users, characteristic of the downlink in a mobile communication system. However, while a lack of synchronicity typically characterizes uplink channels, recent efforts have focused on the creation of synchronicity in the uplink, e.g., [13], [14]. For example, in [14], the China Wireless Telecommunication Standard (CWTS), time division is introduced to support synchronous CDMA uplinks. Our analysis is of course valid for this category of uplinks.

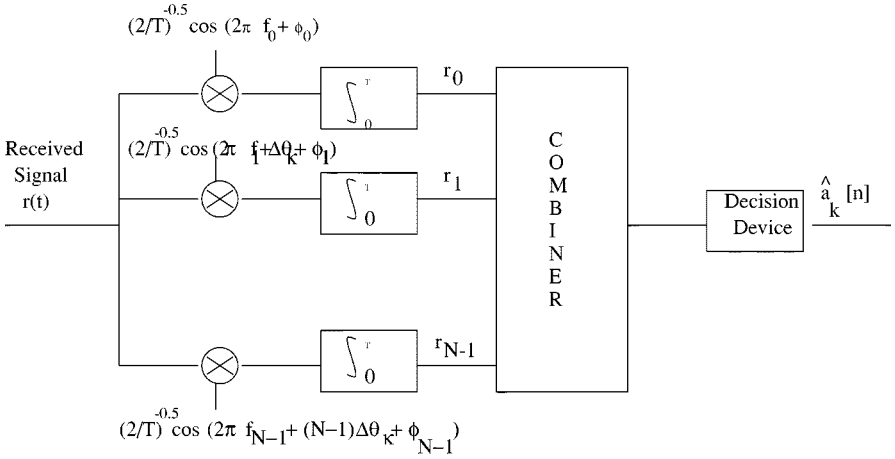

Fig. 3. CI/MC-CDMA receiver for user k.

We address a slowly varying frequency-selective Rayleigh-fading channel. Frequency selectivity refers to the selectivity over the entire bandwidth of transmission and not over each subcarrier transmission; that is [15]

$$1/T_b \ll (\Delta f)_c < BW \tag{7}$$

where $(\Delta f)_c$ is the coherence bandwidth and BW is the total bandwidth of the multicarrier system.

In this work, we examine frequency selectivity resulting in twofold frequency diversity over the entire bandwidth (as in [2]). With N carriers residing over the entire bandwidth, BW, each carrier undergoes a flat fade, with the correlation between the ith subcarrier fade and the jth subcarrier fade characterized by [16]

$$\rho_{i,j} = \frac{1}{1+((f_i - f_j)/(\Delta f)_c)^2}. \tag{8}$$

Generation of correlated fades has been discussed in [17], [18].

IV. Receiver Structures

The received signal corresponds to

$$r(t) = \sum_{k=1}^{K} \sum_{i=0}^{N-1} \alpha_i a_k[n] \cos(2\pi f_i t + i\Delta\theta_k + \phi_i) \cdot p(t - nT_b) + \eta(t) \tag{9}$$

where α_i is the gain and ϕ_i the phase offset in the ith carrier due to the channel, K is the total number of users utilizing the system and $\eta(t)$ represents additive white Gaussian noise (AWGN).

The CI/MC-CDMA receiver for user k is shown in Fig. 3. Here, the received signal is projected onto the orthonormal carriers of the transmitted signal, outputting $\underline{r} = (r_0, r_1, \ldots, r_{N-1})$ where

$$r_i = \alpha_i a_k[n] + \sum_{j=1,\, j\neq k}^{K} \alpha_i a_j[n] \cdot \cos(i(\Delta\theta_j - \Delta\theta_k)) + \eta_i \tag{10}$$

where η_i is a Gaussian random variable with mean 0 and variance $N_o/2$ and exact phase and frequency synchronization has been assumed in determining (10). Next, a suitable combining strategy is used to create a decision variable, D, which then enters a decision device with output $\hat{a}_k[n]$. While different combining methods may be used, minimum mean square error combining (MMSEC) produces the best performances in MC-CDMA [2]. Employing MMSEC in CI/MC-CDMA results in the decision variable (see Appendix A)

$$D = \sum_{i=0}^{N-1} r_i \cdot \left[\frac{\alpha_i}{(R_i\alpha_i^2 + N_o/2)}\right] \tag{11}$$

where R_i is a known constant for a given K and carrier i and corresponds to

$$R_i = \sum_{j=1}^{K} \cos(i(\Delta\theta_j - \Delta\theta_k))^2. \tag{12}$$

It is important to note that by constructing a receiver that processes the signal in the frequency domain rather than in the time domain, we circumvent the need for subchip synchronism.

V. Performance Results

A. Perfect Synchronization

Fig. 4 presents the average bit error rate (BER) versus number of users for $N = 32$ carriers, $SNR = 14$ dB and MMSE combining. Results are presented for a frequency selective Rayleigh-fading channel with $(\Delta f)_c/BW = 0.5$ (supporting twofold diversity over the entire bandwidth).

In Fig. 4, two MC-CDMA curves are also provided, the first assuming orthogonal Hadamard–Walsh (HW) codes of length 32 (dashed line) and the second assuming Gold codes (solid line)—here, length 31 Gold codes support 33 users, with a second set of Gold codes used to support additional users. Additionally, a flat dotted line is drawn, which represents the matched filter lower bound (performance of a single user system exploiting the available diversity through MRC) [19].

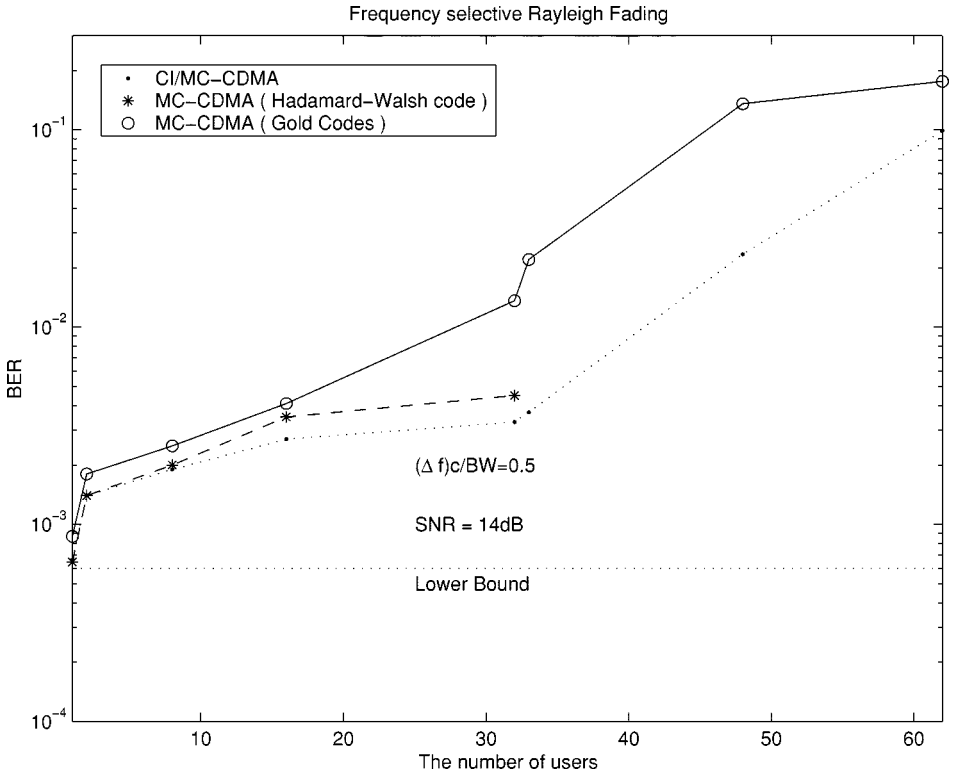

Fig. 4. Average BER performance of CI/MC-CDMA, orthogonal MC-CDMA, and pseudo-orthogonal MC-CDMA.

CI/MC-CDMA BERs (dotted line) match those of orthogonal MC-CDMA up to 32 users. While orthogonal MC-CDMA can not support additional users, CI/MC-CDMA is shown to accommodate an additional 30 users (up to 62 users). If MC-CDMA is preselected to support additional users, by use of pseudo-orthogonal Gold codes, it results in significant performance degradation relative to CI/MC-CDMA as shown by the solid line. In fact, at a BER of 0.0025 the CI/MC-CDMA system supports 32 users, four times the number of users supported by the pseudo-orthogonal MC-CDMA system.

It is observed that with a total of 48 users (32 orthogonal and 16 pseudo orthogonal), CI/MC-CDMA systems offer an average performance comparable to that of MC-CDMA (employing Gold codes with 34 users). Hence, CI/MC-CDMA supports approximately 50% gains in capacity relative to pseudo-orthogonal MC-CDMA methods.

Compared with orthogonal MC-CDMA, CI/MC-CDMA offers the performance of orthogonal MC-CDMA with the flexibility (in terms of number of users) of nonorthogonal MC-CDMA. Compared to nonorthogonal MC-CDMA methods, CI/MC-CDMA significantly enhances performance, with 50% capacity gains observed. Furthermore, the CI/MC-CDMA system is implemented using FFTs and IFFTs similar to MC-CDMA resulting in comparable complexities.

B. Phase Jitter

The channel introduces a phase offset on the ith carrier, ϕ_i, which may be tracked and accounted for at the receiver using a phase locked loop (PLL). Tracking loops are not perfect and, hence, a degradation in performance may result due to phase jitter.

If $\hat{\phi}_i$ is the estimate of the phase using a PLL, then $\theta_i = \phi_i - \hat{\phi}_i$, the carrier phase error, has the Tikhonov probability density function (pdf) [20]

$$p(\theta_i) = \frac{\exp(\rho \cos\theta_i)}{2\pi I_0(\rho)}, \qquad |\theta_i| \le \pi. \tag{13}$$

Here ρ is a parameter related to the tracking loop SNR and $I_0(x)$ is the modified bessel function of the first kind. For first-order tracking loops, ρ is the loop SNR and for second-order loops, ρ is approximately the loop SNR for sufficiently large values [21].

After demodulating the received signal using phase $\hat{\phi}_i$ on the ith carrier, the received signal component r_i [shown in [10] with perfect synchronization] is now given by

$$r_i = \alpha_i a_k[n]\cos\theta_i + \sum_{j=1,\, j\neq k}^{K} \alpha_i a_j[n] \cdot \cos\left(i(\Delta\theta_j - \Delta\theta_k) + \theta_i\right) + \eta_i \tag{14}$$

where $\theta_i = \phi_i - \hat{\phi}_i$. As in Section IV, these signal components are then combined across carriers using the MMSEC of equation (11).

The performance of CI/MC-CDMA with phase jitter is illustrated in Fig. 5. This figure represents simulation results under conditions identical to those used to achieve Fig. 4, with the exception of phase jitters corresponding to $\rho = 10, 30$ and 100 (i.e., rms phase jitters of 18.7°, 10° and 5° respectively). CI/MC-CDMA demonstrates graceful performance degradation, even as phase jitters grow very large. This results because the spreading sequence of user k

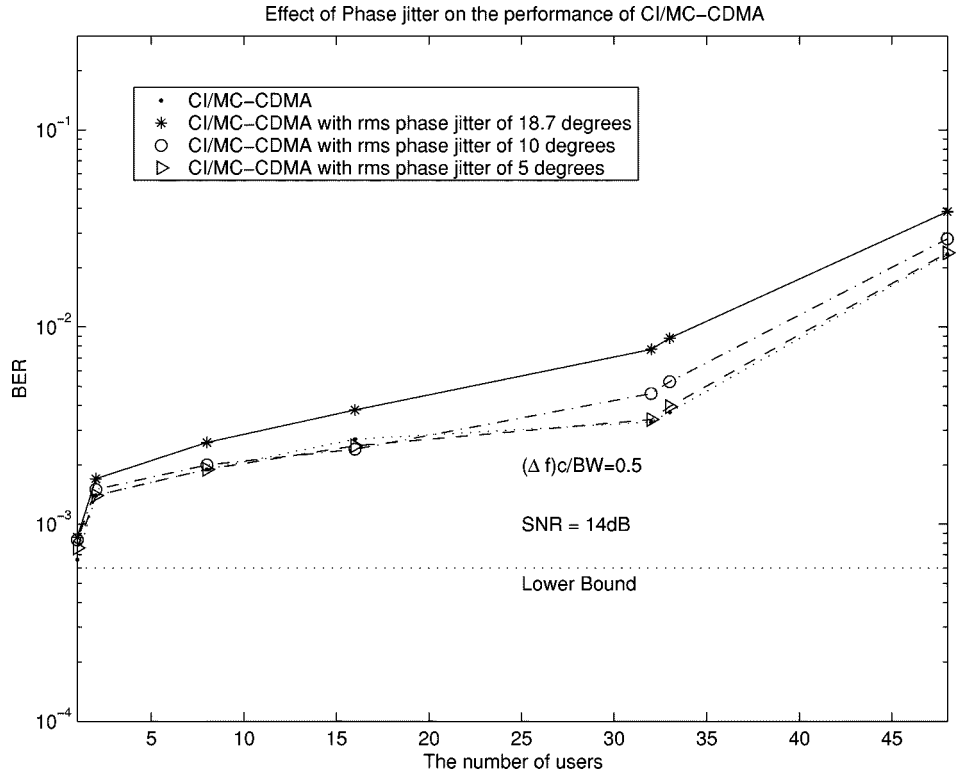

Fig. 5. BER performance of CI/MC-CDMA in the presence of phase jitter.

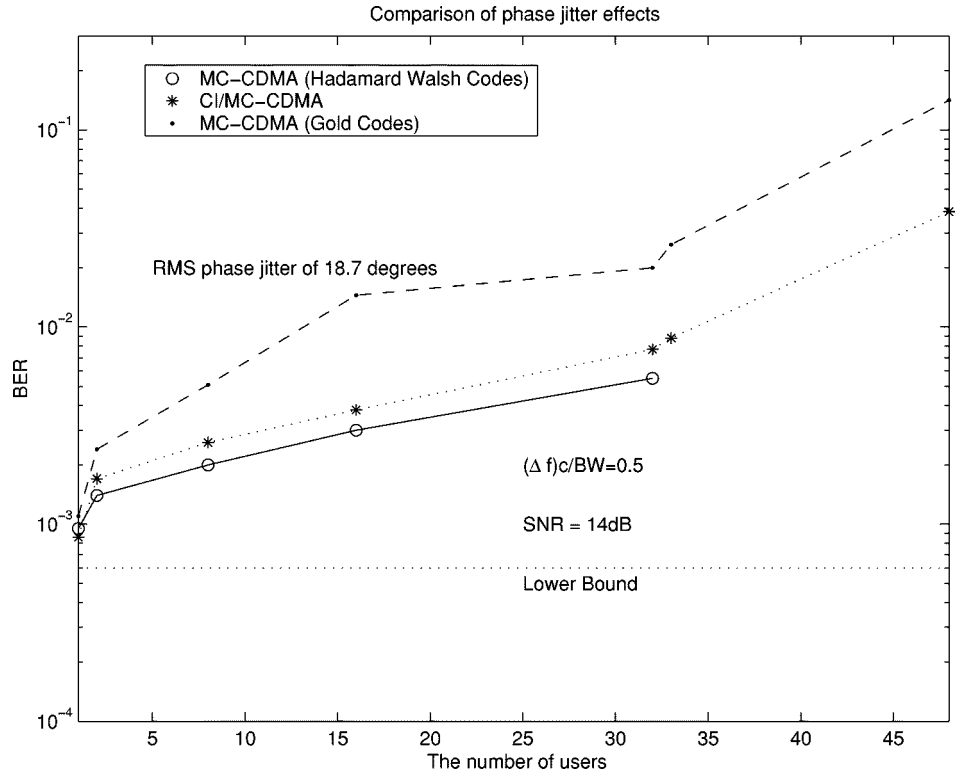

Fig. 6. BER performance comparison of CI/MC-CDMA, orthogonal MC-CDMA and pseudo-orthogonal MC-CDMA in the presence of phase jitter ($\rho = 10$).

is $(1, e^{j\Delta\theta_k}, e^{j2\Delta\theta_k}, \ldots, e^{j(N-1)\Delta\theta_k})$ while user j's code is $(1, e^{j\Delta\theta_j}, e^{j2\Delta\theta_j}, \ldots, e^{j(N-1)\Delta\theta_j})$ and, hence, even if the value of $\Delta\theta_k$ is close to $\Delta\theta_j$ (e.g., $\Delta\theta_k - \Delta\theta_j = \epsilon$), the phase spacing between the ith spreading sequence elements is $i(\Delta\theta_k - \Delta\theta_j)$ (i.e., $i \cdot \epsilon$) which is large for large values of i. Thus, the CI/MC-CDMA system is more robust to phase jitters than one might expect at initial glance.

Figs. 6 and 7 compare the effect of phase jitters on CI/MC-CDMA and MC-CDMA with HW and Gold codes. Fig. 6 shows the performance with phase jitter corresponding

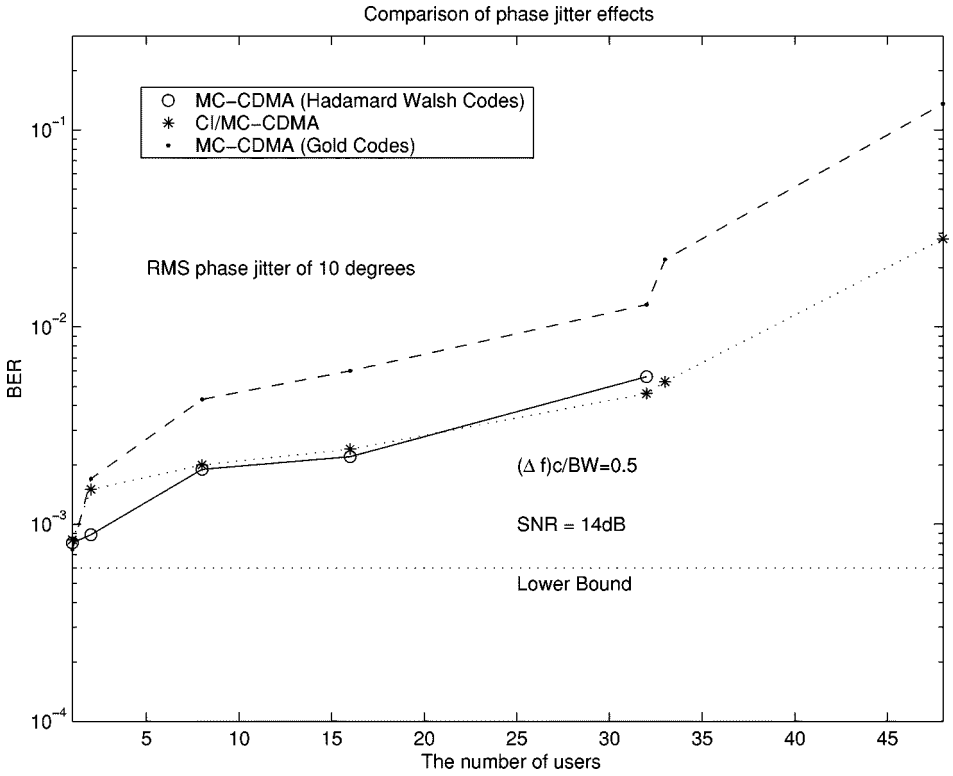

Fig. 7. BER performance comparison of CI/MC-CDMA, orthogonal MC-CDMA and pseudo-orthogonal MC-CDMA in the presence of phase jitter ($\rho = 30$).

to $\rho = 30$ and Fig. 7 shows $\rho = 10$ results. It is observed that relative performance does not change significantly for high values of ρ . As ρ decreases (i.e., as tracking loop SNR degrades), the CI/MC-CDMA degrades at a slightly more rapid rate than its MC-CDMA counterpart, but still offers comparable benefits to those outlined in Section V-A.

C. Frequency Offset

Multicarrier transmission schemes are particularly susceptible to performance degradations from carrier frequency offset. Two major factors are at the root of such carrier frequency offsets: 1) Doppler spread caused by a high-speed mobile and 2) offsets between the oscillator in the transmitter and that of the receiver.

Frequency offsets caused by less than perfect synchronicity between the transmitter and the receiver oscillators are present in the same degree in all subcarriers. On the other hand, offsets due to Doppler spreads are different on each carrier depending on the carrier's location in the spectrum. However, for mobile communication systems operating at a typical carrier frequency of 2 GHz and occupying a characteristic 1-MHz bandwidth, the maximum difference in Doppler spread among 32 carriers is in the range of 0–5 Hz, which is negligible when compared to subcarrier spacings of about 30 KHz [22]. Hence, we treat frequency offsets as a phenomenon identical in all subchannels.

Frequency offsets in an CI/MC-CDMA system results in two key adverse effects. First is the reduction of desired signal amplitude and second is the loss of carrier orthogonality which leads to the generation of intercarrier interferences.

If Δ is the normalized frequency offset (defined as the ratio of the actual frequency offset to the subcarrier separation Δf), the decision variable for the kth user after MMSEC is given by (analogous to [23], [24])

$$D = S + \text{MAI} + \text{ICI}_1 + \text{ICI}_2 + \text{AWGN} \tag{15}$$

where the five components correspond to

$$S = \frac{\sin \pi\Delta}{\pi\Delta} a_k[n] \sum_{i=0}^{N-1} \left[\frac{\alpha_i^2}{(R_i\alpha_i^2 + N_o/2)}\right] \tag{16}$$

$$\text{MAI} = \frac{\sin \pi\Delta}{\pi\Delta} \sum_{i=0}^{N-1} \sum_{j=1,\, j\neq k}^{K} \left[\frac{\alpha_i^2}{(R_i\alpha_i^2 + N_o/2)}\right] \cdot a_j[n] \cdot \cos(i(\Delta\theta_j - \Delta\theta_k)) \tag{17}$$

$$\text{ICI}_1 = \frac{\sin \pi\Delta}{\pi} \sum_{i=0}^{N-1} \sum_{m=0,\, m\neq i}^{N-1} \left[\frac{\alpha_m^2}{(R_m\alpha_m^2 + N_o/2)}\right] \cdot a_k[n] \cos(\Delta\theta_k(i-m)) \frac{1}{\Delta + i - m} \cdot \cos(\phi_m - \phi_i) \tag{18}$$

$$\text{ICI}_2 = \frac{\sin \pi\Delta}{\pi} \sum_{i=0}^{N-1} \sum_{m=0,\, m\neq i}^{N-1} \sum_{j=1,\, j\neq k}^{K} \cdot \left[\frac{\alpha_m^2}{(R_m\alpha_m^2 + N_o/2)}\right] \cdot a_j[n] \cdot \cos(m\Delta\theta_j - i\Delta\theta_k) \frac{1}{\Delta + i - m} \cdot \cos(\phi_m - \phi_i) \tag{19}$$

$$\text{AWGN} = \sum_{i=0}^{N-1} \eta_i \left[\frac{\alpha_i}{(R_i\alpha_i^2 + N_o/2)}\right]. \tag{20}$$

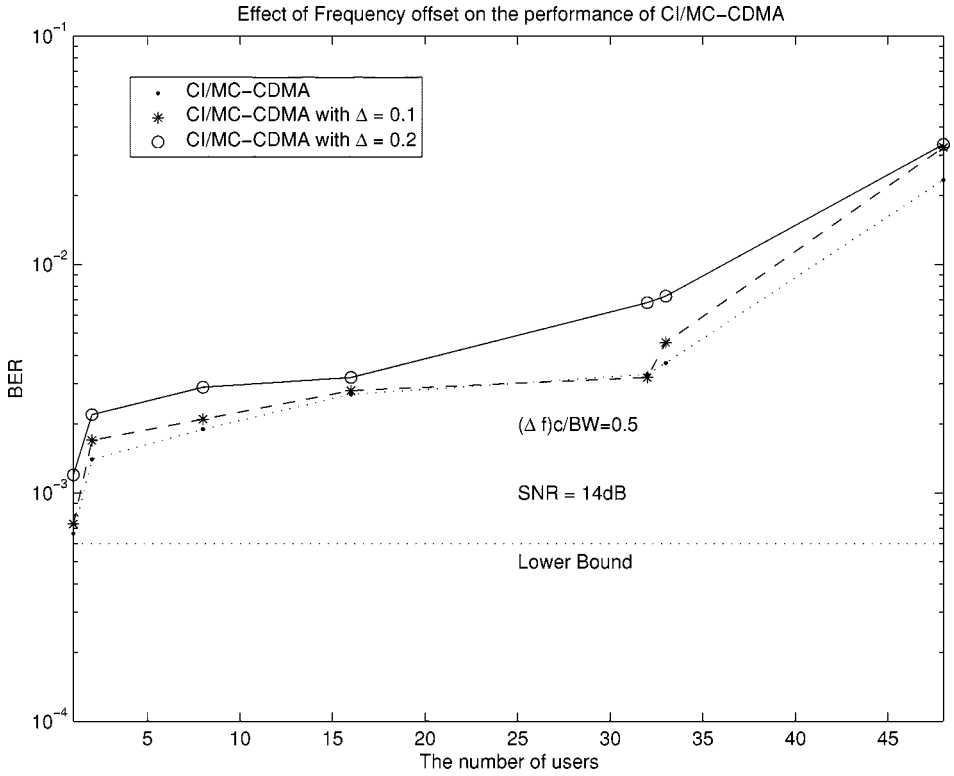

Fig. 8. BER performance of CI/MC-CDMA in the presence of frequency offset.

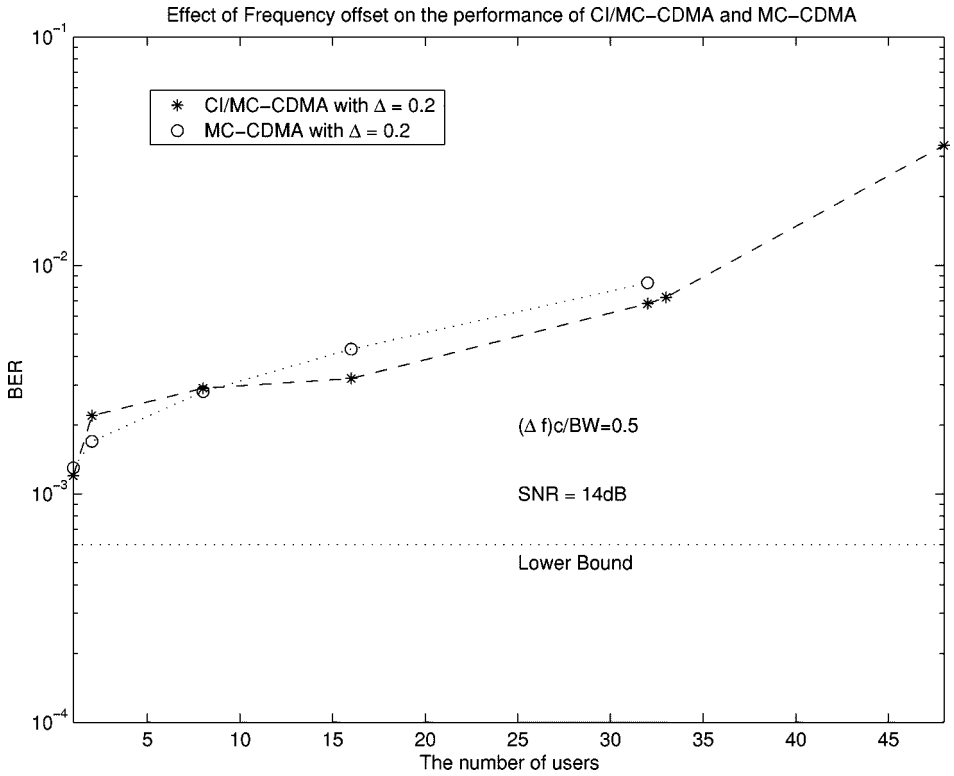

Fig. 9. BER comparison of CI/MC-CDMA and MC-CDMA in the presence of frequency offset ($\Delta = 0.1$).

Here, S, MAI, ICI_1, ICI_2 denote the desired signal, the multi-access interference, the intercarrier interference generated from within the kth user's CI code, and the intercarrier interference generated from the CI codes of the other users.

Fig. 8 plots the performance of CI/MC-CDMA in the presence of frequency offsets $\Delta = 0.1$ and 0.2. It is observed that CI/MC-CDMA is immune to 10% frequency offset while a degradation is visible for a 20% offset level. Figs. 9 and 10 compare the impact of frequency offset on CI/MC-CDMA and tradi-

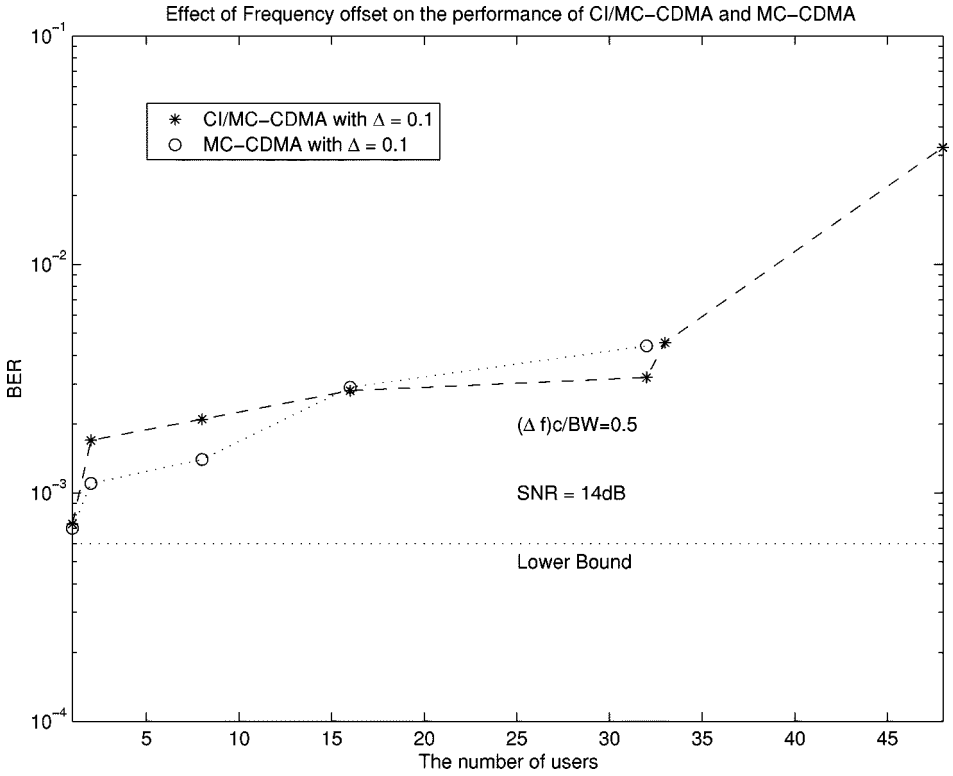

Fig. 10. BER comparison of CI/MC-CDMA and MC-CDMA in the presence of frequency offset ($\Delta = 0.2$).

tional MC-CDMA with HW codes. Both systems are degraded by a comparable amount, demonstrating that CI/MC-CDMA is no more susceptible to frequency offsets than its traditional MC-CDMA counterpart.

VI. Conclusion

In this paper, CI/MC-CDMA, an innovation in MC-CDMA, is introduced. In synchronous frequency selective Rayleigh-fading channels, CI/MC-CDMAs performance matches that of orthogonal MC-CDMA using Hadamard–Walsh codes up to the MC-CDMA $K = N$ user limit; moreover, CI/MC-CDMA provides the added flexibility of supporting $K > N$ (up to $K = 2N - 1$) users by adding users with pseudo orthogonal signature waveforms. When compared to MC-CDMA schemes capable of supporting greater than N users, CI/MC-CDMAs performance exceeds that of MC-CDMA, offering 50% gains in capacity. CI/MC-CDMA also provides added flexibility in the choice of N [$N \in I$ versus $N = 2^n$ or $N = 2^n \pm 1$ ($n \in I$)] making it more robust to the wide range of mobile system applications. The CI/MC-CDMA system was tested in the presence of phase jitters and frequency offsets and was found to demonstrate very graceful degradations in performance at high levels of synchronization errors. Moreover, the effect of phase and frequency jitters on CI/MC-CDMA was found to be comparable to that of a standard MC-CDMA systems.

Some topics of future research include: 1) performance analysis of CI/MC-CDMA system in asynchronous uplink channels and 2) determining optimal phase offsets to be used in polyphase coded subcarriers to reduce PAPR and dynamic range.

Appendix A

The minimum mean square error combining method estimates the transmitted symbol $a_k[n]$ by the linear sum

$$D = \sum_{i=0}^{N-1} w_i r_i. \tag{21}$$

Based on the MMSEC criterion, the estimation error must be orthogonal to all the baseband components of the received subcarriers [25]. Thus

$$E\left\{\left(a_k[n] - \sum_{i=0}^{N-1} w_i r_i\right) \cdot r_i\right\} = 0$$
$$i = 0, 1, \ldots, N-1. \tag{22}$$

The solution to equation (22) as obtained from Weiner filter theory corresponds to [26]

$$w_i = C^{-1} A \tag{23}$$

where $C = E\{r_i r_i | \alpha_i\}$ and $A = E\{a_k[n] r_i | \alpha_i\}$ where $E\{\cdot\}$ denotes the expected value. This operation, when applied to the r_i in CI/MC-CDMA yields

$$C = \alpha_i^2 \sum_{j=1}^{K} \cos(i(\Delta\theta_j - \Delta\theta_k))^2 + N_o/2 \tag{24}$$

$$A = \alpha_i. \tag{25}$$

Substituting (24) and (25) in (23) we obtain the weights for MMSEC

$$w_i = \frac{\alpha_i}{\left(\alpha_i^2 \sum_{j=1}^{K} \cos(i(\Delta\theta_j - \Delta\theta_k))^2 + N_o/2\right)} \tag{26}$$

and, hence, from (21)

$$D = \sum_{i=0}^{N-1} \frac{\alpha_i}{\left(\alpha_i^2 \sum_{j=1}^{K} \cos(i(\Delta\theta_j - \Delta\theta_k))^2 + N_o/2 \right)} \cdot r_i. \quad (27)$$

REFERENCES

[1] N. Yee, J. P. Linnartz, and G. Fettweis, "Multi-carrier CDMA in indoor wireless radio," in *Proc. PIMRC '93*, Yokohama, Japan, Dec. 1993, pp. 109–113.

[2] S. Hara and R. Prasad, "Overview of multi-carrier CDMA," *IEEE Commun. Mag.*, vol. 35, no. 12, pp. 126–133, Dec. 1997.

[3] W. H. Steel, *Interferometry*, 1st ed. Cambridge, U.K.: Cambridge Univ. Press, 1967.

[4] I. Opperman and B. S. Vucetic, "Complex spreading sequences with a wide range of correlation properties," *IEEE Trans. Commun.*, vol. 45, pp. 365–375, Mar. 1997.

[5] G. W. Wornell, "Spread-signature CDMA: Efficient multi-user communication in the presence of fading," *IEEE Trans. Inform. Theory*, vol. 41, no. 5, pp. 1418–1438, Sept. 1995.

[6] ——, "Emerging applications of multirate signal processing and wavelets in digital communications," *Proc. IEEE*, vol. 84, pp. 586–603, Apr. 1996.

[7] A. N. Akansu *et al.*, "Wavelet and subband transforms: Fundamentals and communication applications," *IEEE Commun. Mag.*, pp. 104–115, Dec. 1997.

[8] B. M. Popovic, "Spreading sequences for multicarrier CDMA systems," *IEEE Trans. Commun.*, vol. 47, pp. 918–926, June 1999.

[9] K. Fazel and S. Kaiser, "Analysis of nonlinear distortions on MC-CDMA," in *Proc. 1998 IEEE Int. Conf. Communications*, vol. 2, Atlanta, GA, June 1998, pp. 1028–1034.

[10] G. Redaelli *et al.*, "Analysis of two digital adaptive pre-correctors for nonlinearity in OFDM systems," in *Proc. 1999 IEEE Int. Conf. Communications*, vol. 1, Vancouver, BC, Canada, June 1999, pp. 172–177.

[11] E. Van der Ouderaa, J. Schoukens, and J. Renneboog, "Peak factor minimization of input and output signals of linear systems," *IEEE Trans. Instrument. Meas.*, vol. 37, pp. 207–212, June 1988.

[12] V. Aue and G. P. Fettweis, "Multi-carrier spread spectrum modulation with reduced dynamic range," in *Proc. 1993 IEEE Vehicular Technology Conf.*, Secaucus, NJ, May 1993, pp. 914–917.

[13] F. Kleer, S. Hara, and R. Prasad, "Detection strategies and cancellation schemes in a MC-CDMA system," in *CDMA Techniques for Third Generation Mobile Systems*, 1st ed. Norwell, MA: Kluwer, 1999, pp. 185–215.

[14] China Wireless Telecommunications Standard (CWTS), "Physical layer—General description,", TS C101 V3.0.0, 1999.

[15] J. Proakis, *Digital Communications*, 3rd ed. New York: McGraw-Hill, 1995.

[16] W. Xu and L. B. Milstein, "Performance of multicarrier DS CDMA systems in the presence of correlated fading," in *IEEE 47th Vehicular Technology Conf.*, Phoenix, AZ, May 1997, pp. 2050–2054.

[17] R. B. Ertel and J. H. Reed, "Generation of two equal power correlated Rayleigh-fading envelopes," *IEEE Commun. Lett.*, vol. 2, pp. 276–228, Oct. 1998.

[18] B. Natarajan, C. R. Nassar, and V. Chandrasekhar, "Generation of correlated Rayleigh-fading envelopes for spread spectrum applications," *IEEE Commun. Lett.*, vol. 4, pp. 9–11, Jan. 2000.

[19] M. K. Simon and M. S. Alouini, *Digital Communication Over Fading Channels—A Unified Approach to Performance Analysis*. New York: Wiley, 2000.

[20] H. Leib and S. Pasupathy, "Trellis-coded MPSK with reference phase errors," *IEEE Trans. Commun.*, vol. COM-35, Sept. 1987.

[21] W. C. Lindsey and M. K. Simon, *Telecommunication Systems Engineering*. Englewood Cliffs, NJ: Prentice-Hall, 1973.

[22] [23] Y. Kim, S. Choi, C. You, and D. Hong, "Effect of carrier frequency offset on the performance of an MC-CDMA system and its countermeasure using pulse shaping," in *Proc. IEEE Int. Conf. Communications*, vol. 1, Vancouver, Canada, June 1999, pp. 167–171.

[24] P. H. Moose, "A technique for orthogonal frequency division multiplexing frequency offset correction," *IEEE Trans. Communications*, vol. 42, pp. 2908–2914, Oct. 1994.

[25] Leon-Garcia, *Probability and Random Processes for Electrical Engineering*, 2nd ed. Reading, MA: Addison-Wesley, May 1994.

[26] S. Haykin, *Adaptive Filter Theory*, 2nd ed. Englewood Cliffs, NJ: Prentice-Hall, 1991.

Balasubramaniam Natarajan received the B.E. degree in electrical and electronics engineering (with distinction) from Birla Institute of Technology and Science, Pilani, India, in 1997. He is currently working toward the Ph.D. degree at the Department of Electrical and Computer Engineering, Colorado State University, Fort Collins, CO.

He was involved in telecommunications research at Daimler Benz Research Center, Bangalore, India, in early 1997. His current research interests include multiple access techniques, estimation theory, multicarrier modulation, multi-user detection, and channel modeling.

Carl R. Nassar received the B.S degree in 1989, the M.S. degree in 1990, and the Ph.D. degree in 1997, all in electrical engineering with an emphasis on telecommunications from McGill University, Montreal, Canada.

From 1990 to 1991, he was a Design Engineer with CAE Electronics, Montreal, Canada. After 1997, he spent a brief time as an Assistant Professor at McGill University and then accepted a similar position at Colorado State University, Fort Collins, CO. He currently directs the RAWCom (Research in Advanced Wireless Communications) Laboratory, Colorado State University, which focuses on advancements in multiple access technologies using the carrier interferometry approach. He is also the author of *Telecommunications Demystified* (Eagle Rock, VA: LLH Technology, 2001), a technically complete, yet fun-to-read, book explaining the world of telecommunications to engineers.

Steve Shattil received the B.S. degree (physics) from Rensselaer Polytechnic Institute, Troy, NY, the M.S. degree (physics) from the Colorado School of Mines, Golden, and the M.E. degree in electrical engineering from the University of Colorado, Boulder, respectively.

He has a background in optical engineering, which he applies to radio communications. His work includes developing new types of multicarrier signal processing for antenna arrays, spread spectrum protocols, and fiber optics. He is the Chief Scientist and Patent Counsel at Idris Communications Inc., Boulder, CO.

Marco Michelini was born in Pietrasanta, Italy, in 1974. He received the Dr.Ing. degree in telecommunication engineering from the Universita di Firenze, Italy, in 2000. He is currently working toward the Ph.D. degree at the Dipartmento di Electtronica e Telecommunicazioni, Universita di Firenze.

From August 1998 to December 1998, he worked as a Research Assistant at the Electrical and Computer Engineering Department, Colorado State University, Fort Collins, on carrier interferometry topics. His main fields of interest are multicarrier communications, CDMA, multiuser detection techniques, and mobile communication networks.

Zhiqiang Wu was born in 1973. He received the B.S. degree in wireless telecommunications from Beijing University of Posts and Telecommunications, Beijing, China, in 1993 and the M.S. degree in computer signal processing from Peking University, Beijing, China, in 1996. He is currently working toward the Ph.D. degree at the Department of Electrical and Computer Engineering at Colorado State University, Fort Collins, CO.